ESC European Society of Cardiology

Europace (2023) **25**, 478–486
https://doi.org/10.1093/europace/euac220

CLINICAL RESEARCH

The transmural activation interval: a new mapping tool to identify ventricular tachycardia substrates in right ventricular cardiomyopathy

Jeroen Venlet [1], Sebastiaan R. Piers [1], Jarieke Hoogendoorn [1], Alexander F.A. Androulakis[1], Marta de Riva[1], Rob J. van der Geest [2], and Katja Zeppenfeld [1]*

[1]Willem Einthoven Center for Cardiac Arrhythmia Research and Management, Department of Cardiology, Leiden University Medical Centre, PO Box 9600, 2300 RC Leiden, The Netherlands; and [2]Department of Image Processing, Leiden University Medical Centre, PO Box 9600, 2300 RC Leiden, The Netherlands

Received 8 April 2022; accepted after revision 23 October 2022; online publish-ahead-of-print 8 December 2022

Aims In right ventricular cardiomyopathy (RVCM), intramural scar may prevent rapid transmural activation, which may facilitate subepicardial ventricular tachycardia (VT) circuits. A critical transmural activation delay determined during sinus rhythm (SR) may identify VT substrates in RVCM.

Methods and results Consecutive patients with RVCM who underwent detailed endocardial-epicardial mapping and ablation for scar-related VT were enrolled. The transmural activation interval (TAI, first endocardial to first epicardial activation) and maximal activation interval (MAI, first endocardial to last epicardial activation) were determined in endocardial-epicardial point pairs located <10 mm apart. VT-related sites were determined by conventional substrate mapping and limited activation mapping when possible. Nineteen patients (46 ± 16 years, 84% male, 63% arrhythmogenic right ventricular cardiomyopathy, 37% exercise-induced arrhythmogenic remodelling) were inducible for 44 VT [CL 283 (interquartile range, IQR 240–325)ms]. A total of 2569 endocardial-epicardial coupled point pairs were analysed, including 98 (4%) epicardial VT-related sites.

The TAI and MAI were significantly longer at VT-related sites compared with other electroanatomical scar sites [TAI median 31 (IQR 11–50) vs. 2 (−7–11)ms, $P < 0.001$; MAI median 65 (IQR 45–87) vs. 23 (13–39)ms, $P < 0.001$]. TAI and MAI allowed highly accurate identification of epicardial VT-related sites (optimal cut-off TAI 17 ms and MAI 45 ms, both AUC 0.81). Both TAI and MAI had a better predictive accuracy for VT-related sites than endocardial and epicardial voltage and electrogram (EGM) duration (AUC 0.51–0.73).

Conclusion The transmural activation delay in SR can be used to identify VT substrates in patients with RVCM and predominantly hemodynamically non-tolerated VT, and may be an important new mapping tool for substrate-based ablation.

Keywords Arrhythmias • Arrhythmogenic right ventricular cardiomyopathy • Catheter ablation • Transmural activation delay

* Corresponding author. Tel: +31715262020; Fax: +31715266809. *E-mail address* K.Zeppenfeld@lumc.nl

What's new?

- This is the first study to systematically analyse the TAI and MAI during SR in patient with RV cardiomyopathies and predominantly hemodynamically non-tolerated VT.
- TAI and MAI allowed more accurate identification of areas harbouring the VT substrate compared with voltage and EGM duration criteria.
- TAI and MAI are novel tools to identify critical areas for epicardial VT, and may facilitate substrate-based ablation at the epicardial RV.

Introduction

In patients with right ventricular cardiomyopathies (RVCM), ventricular tachycardia (VT) is typically due to scar-related re-entry often confined to the epicardium.[1–5] Ablation of poorly tolerated VT requires a substrate-based ablation strategy. However, voltage mapping to accurately identify subepicardial scar can be hampered by epicardial fat and other anatomical obstacles. Scar-related re-entry is facilitated by areas of functional or fixed conduction block, which may be detectable during sinus rhythm (SR).

In patients with arrhythmogenic right ventricular cardiomyopathy (ARVC), an altered and delayed epicardial RV activation has been reported, compared with patients without structural heart disease.[2] Areas with prolonged transmural activation due to intramural fat and fibrosis may result in protected subepicardial areas which may facilitate re-entry VT.

In the present study, we propose the transmural activation interval (TAI) as a novel parameter reflecting local transmural activation delay or transmural block during SR. We hypothesize that a critically prolonged TAI during SR may identify protected epicardial areas that harbour critical VT isthmus sites in RVCM.

Methods

Patients

Consecutive patients with RVCM who underwent detailed endocardial-epicardial mapping and ablation for scar-related VT between November 2011 and April 2015 were enrolled. Patients with RV pacing during mapping and mechanically induced right bundle branch block during mapping were excluded.

All patients underwent a comprehensive evaluation according to the 2010 revised Task Force criteria of ARVC.[6] Mutations were classified as previously described.[7] The diagnosis of exercise-induced arrhythmogenic remodelling (EIAR) was based on the presence of an isolated RV outflow tract scar responsible for VT in endurance athletes, without evidence for inherited cardiomyopathy/ARVC.[3] The study was approved by the local ethical committee. All patients provided informed consent prior to the mapping and ablation procedure.

Electroanatomical mapping and ablation

All anti-arrhythmic drugs were discontinued for ≥5 half-lives, if possible, with the exception of amiodarone. Before endocardial-epicardial mapping, ECG-gated cardiac computed tomographic (CT) was performed, segmented, and loaded into the mapping system for real-time integration with electroanatomical mapping (EAM) data as previously described.[8,9] Epicardial access was obtained through a subxiphoid puncture if a priori endocardial ablation had failed or an epicardial substrate was suspected based on disease aetiology, endocardial voltage, and/or activation mapping. EAM of the RV endocardium and epicardium was performed during SR using a 3.5 mm irrigated-tip catheter (NaviStar Thermocool, Biosense Webster Inc., Diamond Bar, CA, USA) and the CARTO system. Endocardial mapping was performed using a long steerable sheath (Agilis NxT Steerable Introducer, Abbott, Abbott Park, IL, USA) in all cases to ensure adequate tissue contact. Electrograms (EGMs) were filtered at 30–400 Hz (bipolar) and 1–240 Hz (unipolar). Programmed electrical stimulation was conducted [3–4 drive cycle lengths (CL) (600, 500, 400, 350 ms), 3–4 extra's (≥200 ms)] from at least two RV sites. VT-related sites were identified based on activation and entrainment mapping for hemodynamically tolerated VT, and on combined substrate and pace-mapping (≥11/12 pace-match with a prolonged stim-QRS interval ≥40 ms) for hemodynamically not tolerated VT and targeted by ablation.

At the end of the procedure, the stimulation protocol was repeated. Complete success was defined as non-inducibility of any sustained VT, partial success as inducibility of any non-clinical VT, and failure as inducibility of the clinical VT. The procedural success was categorized as undetermined if no stimulation was performed after ablation.

Patients were followed at the outpatient clinic at 2 and 6 months after ablation and at 6-monthly intervals thereafter. VT recurrence was defined as occurrence of any VT lasting >30 s or terminated by the ICD.

Post-procedural analysis

All bipolar EGMs were displayed at the same gain (Carto caliper 0.14 mV/1 cm) and sweep speed (200 mm/s). Bipolar voltage (BV) > 1.5 mV was considered normal at the endocardium and epicardium. Unipolar voltage (UV) > 3.90 mV was considered normal at the endocardium.[10] EGM duration was measured from the first to the last sharp bipolar peak deflection (SBP). Normal values for epicardial EGM duration were based on the 95th percentile of EGM duration at sites without electroanatomical scar.

The local activation time (LAT) during SR was defined as first sharp peak deflection of the bipolar EGM, which usually coincides with the maximum downstroke of the unipolar EGM (*Figure 1*). For all fragmented EGMs, LAT was also defined as first sharp bipolar peak deflection, since far field components of the unipolar EGM may obscure local activation.

Endocardial-epicardial point pairs

All mapping points were exported and superimposed on the corresponding short-axis CT slice. Local epicardial fat thickness was determined using in-house developed software (Mass, V2013-EXP LKEB, Leiden). In Matlab (software-version 2014b) each endocardial point was linked to the closest epicardial mapping point based on shortest Euclidean distance between the three-dimensional coordinates. The epicardial fat thickness was subtracted from the Euclidean distance between the point pairs to estimate the point distance without the influence of fat. Endocardial and epicardial point pairs with a distance <10 mm apart were selected for analysis to exclude skewed point pairs and septal points. Points pairs without nearfield EGM at either the endocardium or epicardium and points from re-maps after radiofrequency ablation, were excluded from the analysis. Paired points were categorized as:

(i) No scar sites, defined by normal endocardial bipolar and UV
(ii) Scar sites, defined by abnormal endocardial bipolar and/or UV
(iii) Epicardial VT-related sites

Transmural activation interval and maximal activation interval

The TAI as a measure for the transmural activation delay was defined as interval between the earliest endocardial and epicardial LAT at each point pair. The maximal activation interval (MAI) was defined as interval between the endocardial LAT and the latest epicardial sharp deflection, reflecting the combination of both transmural and epicardial inlayer conduction delay (*Figure 1*). The TAI and MAI of epicardial VT-related sites, scar sites, and sites without scar were compared. Only epicardial VT-related sites were selected because of the study hypothesis that a critically prolonged TAI may identify protected epicardial areas with critical VT isthmus sites.

Statistical analysis

Categorical variables are displayed as number (percentage), and continuous variables are expressed as mean ± standard deviation or median (interquartile range, IQR). Continuous variables were compared using the Mann–Whitney *U* Test. The Kaplan–Meier method was used to determine the cumulative VT-free survival. Receiver operating characteristics curve analysis was performed to determine the optimal cut-off value, defined as the value maximizing the sum of sensitivity and specificity. All tests were two-sided and *P*-values <0.05 were considered statistically significant. All analyses were performed with SPSS version 23.0 (IBM SPSS, Armonk, NY, USA).

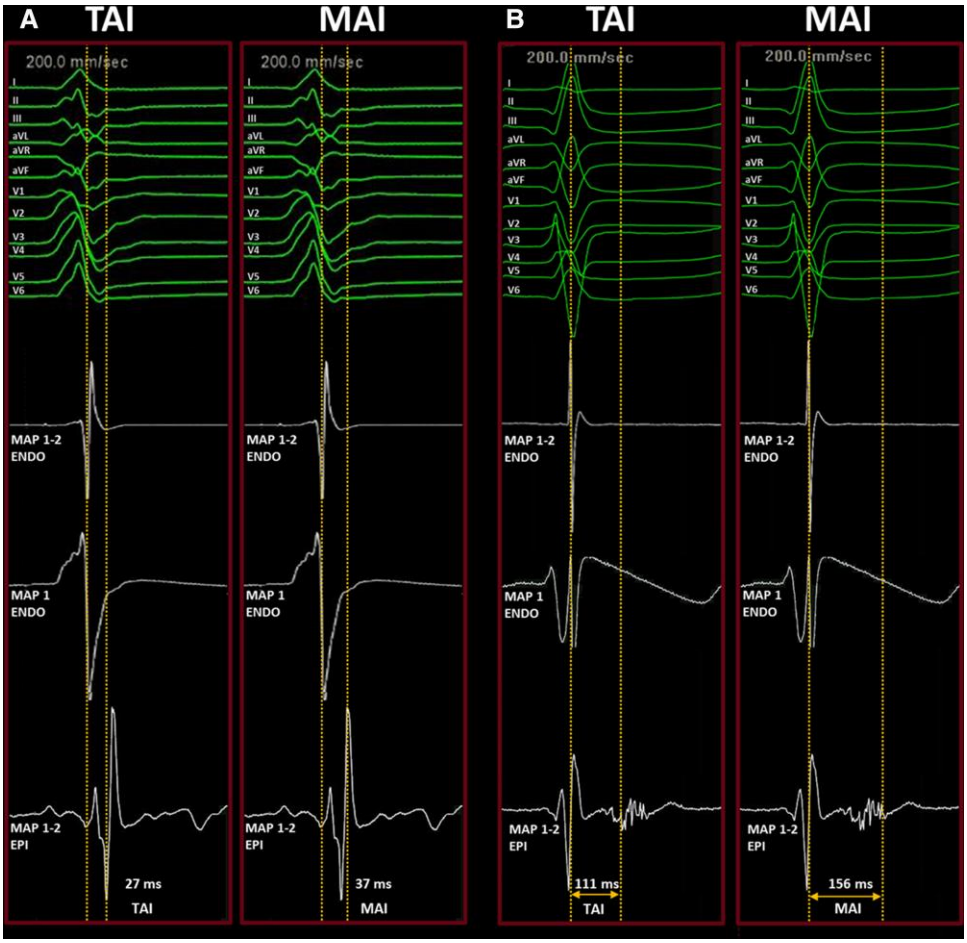

Figure 1 Method. Panel A shows an example of paired points with a prolonged transmural activation interval (TAI) and normal maximal activation interval (MAI) duration. The first sharp bipolar peak deflection (SBP) (MAP 1–2 endo) coincides with the maximal downstroke of the endocardial unipolar signal (MAP 1 endo). Panel B illustrates an example of a prolonged TAI and MAI duration due a transmural and inlayer conduction delay. The first epicardial EGM component coincides exactly with the corresponding endocardial local activation time, and may be considered as farfield signal from the endocardium. The second component is a late and fragmented EGM.

Results

Patients

Out of 21 consecutive patients with RVCM, who underwent endocardial-epicardial mapping and ablation for scar-related VT, one patient was excluded because of RV pacing and one due to mechanically induced right bundle branch block during mapping. The remaining 19 patients (age 46 ± 16 years, 84% male) were enrolled. The underlying aetiology was definite ARVC according to Task Force criteria in 11 (58%), borderline ARVC in one (5%), and EIAR in 7 (37%). In ARVC, a pathogenic ARVC associated mutation was found in 9/12 (75%) patients (desmosomal mutation in 7 and phospholamban mutation in 2). Baseline characteristics are provided in *Table 1*.

Electroanatomical mapping and ablation

The procedure was performed under general anaesthesia in all patients. A total of 44 VT were induced with a median CL of 283 (IQR 240–325) ms. Endo- and epicardial substrate mapping with successful CT integration was performed prior to ablation with a mean of 237 ± 61 mapping points at the RV endocardium and 348 ± 135 at the epicardium (heart rate during mapping 60 ± 18 beats per min). Our substrate mapping approach includes systematical pace-mapping, regardless of the local EGM characteristics. Only 7/44 VTs (16%) in five patients were hemodynamically briefly tolerated; for 6/7 of these VTs, critical VT isthmus sites could be determined based on concealed entrainment and/or VT slowing and termination during ablation. For 31/44 VTs (70%) in 17 patient's, VT-related sites were identified by conventional substrate mapping and pace-mapping.

At the epicardium, a median of 11 (IQR 8–19) RF-applications per patient was delivered. At the endocardium, only limited ablation was performed (median of 1 (IQR 0–9).

The acute outcome was complete success in 14 (74%) patients, partial success in 4 (21%), and undetermined in 1 (5%). During a median follow-up of 48 (IQR 5–59) months, 8 (42%) patients experienced a VT recurrence. VT-free survival was 61% at 24 months. There were no procedure related complications.

Coupled point pairs

A total of 4479 endocardial mapping points were coupled to epicardial points. After exclusion of all point pairs with a distance >10 mm, points from re-maps, and points without near field EGM, 2569 point pairs were

selected for analysis. Of the 2569 paired points, 1186 (46%) paired points were categorized as 'no scar', 1285 (50%) as 'scar', and 98 (4%) point pairs as 'epicardial VT-related site' location. Median epicardial EGM duration was 18 (IQR 12–27) ms. At sites without electroanatomical scar, EGM duration of the epicardial points was 16 (IQR 10–23) ms, 95% of the points had an EGM duration ≤43 ms, which was considered normal.

Transmural activation interval, maximal activation interval, and electrogram characteristics at ventricular tachycardia -related sites, EA scar sites, and no scar sites

Details of the EGM characteristics, MAI, and TAI at VT-related sites, scar sites, and normal points are provided in *Table 2*.

Table 1 Baseline characteristics

	ARVC ($n = 12$)	EIAR ($n = 7$)
Age, years	47 ± 16	44 ± 16
Sex (male)	10 (83%)	6 (86%)
BMI, kg/m^2	25 ± 4	23 ± 3
ARVC 2010 TFC		
Imaging criteria		
Major	7 (58%)	0 (0%)
Minor	0 (0%)	0 (0%)
ECG depolarization criteria		
Major	3 (25%)	0 (0%)
Minor	5 (42%)	0 (0%)
ECG repolarization criteria		
Major	6 (50%)	0 (0%)
Minor	3 (25%)	1 (14%)
Pathogenic mutation		
Desmosomal	7 (58%)	0 (0%)
Any ARVC associated	9 (75%)	0 (0%)

Variables are expressed as mean ± SD or number (percentage). ARVC denotes arrhythmogenic right ventricular cardiomyopathy; EIAR, exercise-induced arrhythmogenic remodelling; TFC, task force criteria.

The median endocardial BV at paired points was 2.7 (IQR 1.2–4.6) mV. The endocardial BV did not differ between epicardial VT-related sites and other epicardial scar sites ($P = 0.856$). In contrast, the endocardial UV and epicardial BV were significantly lower at VT-related sites compared with other scar sites ($P = 0.002$ and $P < 0.001$, respectively). The epicardial EGM duration was significantly longer at VT-related sites compared with other scar sites [34 (IQR 21–42) vs. 20 (IQR 12–30) ms, respectively, $P < 0.001$]. However, the epicardial EGM duration was normal at 78% of all VT-related sites.

The median TAI of all paired points was 3 (IQR −4–11) ms. At epicardial VT-related sites, the median TAI was 31 (IQR 11–50) ms and significantly longer compared with scar points not related to VT [median 2 (IQR −7–11) ms, $P < 0.001$], *Table 2*, *Figures 2–4*. The median MAI was 22 (IQR 14–34) ms. At VT-related sites, the MAI was significantly longer and showed no overlapping IQR, if compared with scar sites not related to VT [median 65 (IQR 45–87) vs. 23 (IQR 13–39) ms, respectively, $P < 0.001$].

At sites with either concealed entrainment or VT slowing and termination during ablation, the median TAI was 35 (range 34–185) ms, and the median MAI was 63 (range 34–197) ms.

Diagnostic accuracy for ventricular tachycardia-related sites

Endocardial bipolar and UV did not allow to distinguish between VT-related sites and other scar sites (AUC 0.51 and AUC 0.59, respectively, *Table 3*).

The epicardial BV and EGM duration had a moderate diagnostic accuracy to detect VT-related sites (epicardial BV AUC 0.73, cutoff 0.4 mV, sensitivity 66%, specificity 71%; epicardial EGM duration AUC 0.66, cutoff 34 ms, sensitivity 54%, specificity 79%, respectively).

TAI and MAI were superior to other parameters to distinguish between epicardial VT-related sites and other scar sites (*Table 3*). The optimal TAI cutoff to differentiate between VT-related sites and other scar sites was 17 ms (AUC 0.81, sensitivity 75%, specificity 84%, *Table 3* and *Figures 2–4*). The optimal MAI cutoff to differentiate between VT-related sites and other scar sites was 45 ms (AUC 0.81, sensitivity 77%, specificity 80%). The TAI was >17 ms at all sites with either concealed entrainment or VT slowing and termination during ablation. The MAI was >45 ms at 4/6 (67%) of these sites.

Transmural activation interval in arrhythmogenic right ventricular cardiomyopathy and exercise-induced arrhythmogenic remodelling

Of the 2569 point pairs, 1664 were obtained in patients with ARVC and 905 in patients with EIAR. Of the 1664 paired points in ARVC patients,

Table 2 EGM characteristics and TAI and MAI according to points categories

	No scar ($n = 1186$)	Scar sites ($n = 1285$)	Epicardial VT-related sites ($n = 98$)	*P*-value[a]
All patients				
Endocardial BV, mV	4.5 (3.1–6.3)	1.3 (0.5–2.4)	1.1 (0.5–2.7)	0.856
Endocardial UV, mV	6.2 (5.1–7.8)	2.2 (1.5–3.1)	1.7 (1.1–2.9)	0.002
Epicardial BV, mV	1.4 (0.8–2.5)	0.6 (0.3–1.3)	0.3 (0.1–0.5)	<0.001
Epicardial EGM duration, ms	16 (10–23)	20 (12–30)	34 (21–42)	<0.001
TAI, ms	4 (−2–9)	2 (−7–11)	31 (11–50)	<0.001
MAI, ms	21 (14–29)	23 (13–39)	65 (45–87)	<0.001

Variables are expressed as median (IQR). BV denotes bipolar voltage; MAI, maximal activation interval; TAI, transmural activation interval; UV, unipolar voltage.
[a]For differentiation between epicardial VT-related sites and scar sites.

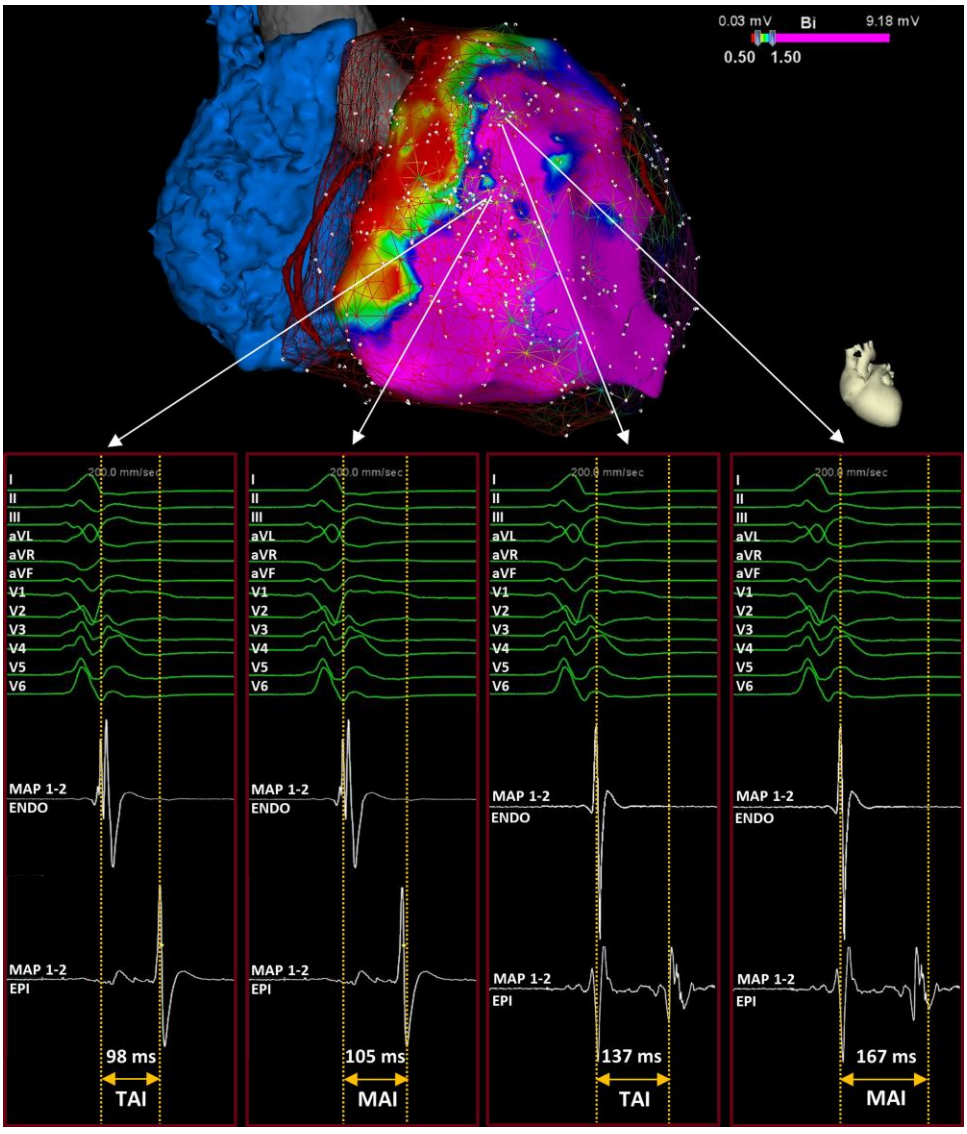

Figure 2 Prolonged TAI in an ARVC patient. An endocardial electroanatomical map is colour coded for bipolar voltage (BV), and the corresponding epicardial BV map is displayed in a mesh view to show the proximity of coupled endocardial and epicardial point pairs. Also, the CT derived cardiac anatomy is integrated with the electroanatomical maps. The lower panels show the transmural activation measurements at two coupled point pairs with the endocardial (MAP 1–2 ENDO) and epicardial (MAP 1–2 EPI) bipolar electrograms. The left two panels show a prolonged transmural activation interval (TAI) and a similarly prolonged maximal activation interval (MAI) due to a prolonged transmural activation delay, without significant inlayer activation delay. The right two panels show a prolonged TAI and a further prolonged MAI due to a combination of transmural and inlayer activation delay.

556 (33%) fulfilled the electroanatomical criteria for no scar, 1024 (62%) were scar sites and 84 (5%) pairs included an epicardial VT-related site. The median TAI at epicardial VT-related sites [26 (IQR 7- 49) ms] was significantly longer compared with other scar sites [3 (IQR −7–12) ms, *P*-value <0.001, *Table 4*]. The MAI was also significantly longer at VT-related sites vs. scar sites [63 (IQR 38–85) vs. 22 (IQR 12–37) ms, respectively, *P*-value <0.001]. In ARVC, both, the TAI and MAI had a good diagnostic accuracy for VT-related sites (AUC 0.78 and 0.80, respectively, *Table 4*).

In patients with EIAR, 905 paired point pairs were subdivided in 630 normal points (70%), 261 scar sites (29%), and 14 epicardial VT-related sites (2%). In patients with EIAR, all VT-related sites and all sites with abnormal TAI and MAI were confined to the epicardial RVOT. The median TAI at epicardial VT sites [44 (IQR 30–75) ms] was significantly longer compared with scar sites (2 [IQR −6–7] ms, *P*-value <0.001, *Table 4*). Similarly, the MAI was significantly longer at VT-related sites vs. scar sites [86 (IQR 47–113) vs. 26 (IQR 16–44) ms, respectively, *P*-value <0.001]. Of interest, in EIAR, both TAI and MAI had an excellent diagnostic accuracy for VT-related sites (AUC 0.99 and 0.91, respectively, *Table 4*).

Of note, at VT-related sites, both TAI and MAI were significantly longer in EIAR compared with ARVC patients ($P = 0.016$ and $P = 0.037$, respectively).

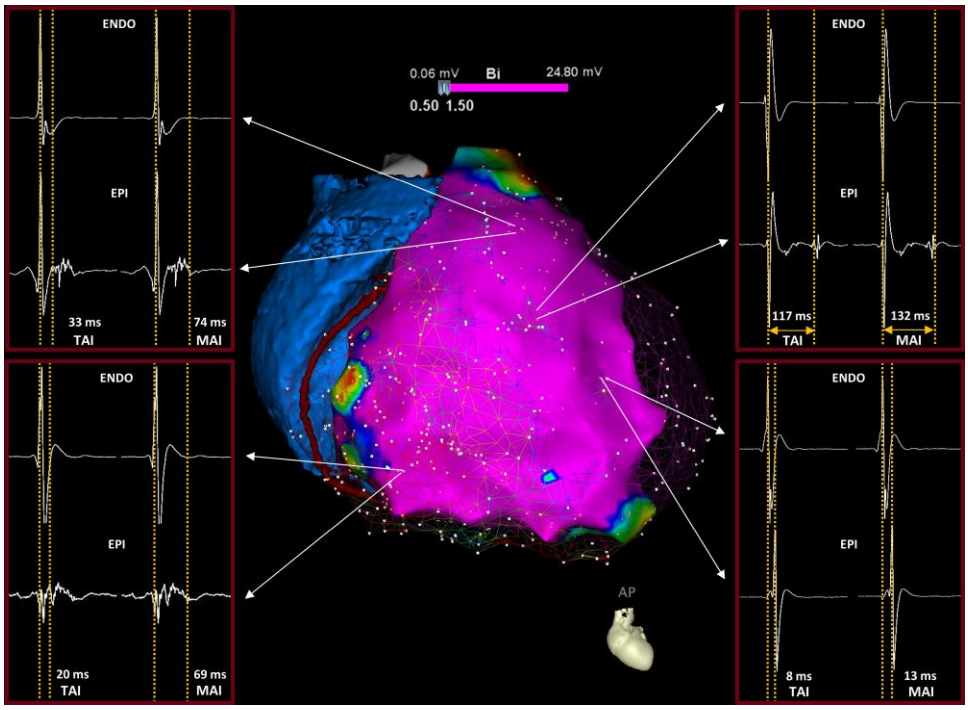

Figure 3 Examples of prolonged TAI and MAI in ARVC patient. Electroanatomical endocardial bipolar voltage (BV) map and epicardial BV map displayed in a mesh view of a patient with ARVC with four examples of coupled points pairs with the endocardial (MAP 1–2 ENDO) and epicardial (MAP 1–2 EPI) bipolar electrograms and the local transmural activation interval (TAI) and maximal activation interval (MAI). Right upper panel: prolonged TAI and MAI due to a transmural activation delay; lower right: normal TAI and MAI; both left examples: prolonged TAI and MAI due to a combined transmural and inlayer activation delay.

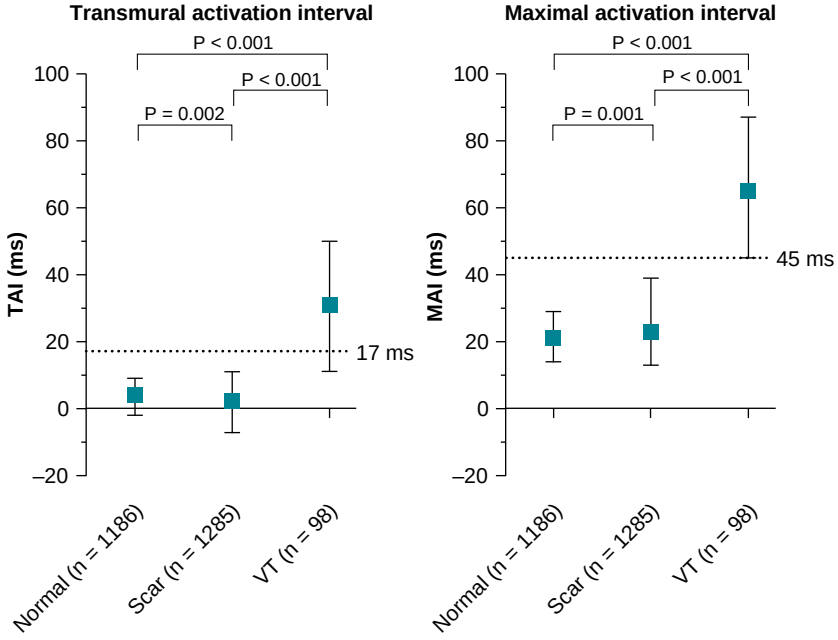

Figure 4 Transmural activation interval and VT-related sites. Median and interquartile range for transmural activation interval (TAI) and maximal activation interval (MAI) for the three different point categories. VT-related sites (VT) had a longer TAI and MAI duration compared with normal points and scar points. The optimal cutoff between VT-related sites and scar sites is depicted by the dashed black line.

Table 3 EGM characteristics and TAI and MAI to detect VT-related sites

	Optimal cutoff[a]	AUC (95% CI)[a]	Sensitivity[a]	Specificity[a]
All patients				
Endocardial BV, mV	1.1	0.51 (0.44–0.57)	50%	59%
Endocardial UV, mV	1.5	0.59 (0.53–0.66)	48%	75%
Epicardial BV, mV	0.4	0.73 (0.68–0.78)	66%	71%
Epicardial EGM duration, ms	34	0.66 (0.60–0.72)	54%	79%
TAI, ms	17	0.81 (0.75–0.86)	75%	84%
MAI, ms	45	0.81 (0.77–0.85)	77%	80%

Variables are expressed as median (IQR). BV denotes bipolar voltage; CI, confidence interval; MAI, maximal activation interval; TAI, transmural activation interval; UV, unipolar voltage.
[a]For differentiation between epicardial VT-related sites and scar sites

Table 4 TAI and MAI in ARVC and EIAR and optimal cutoff for TAI and MAI to detect VT-related sites

	No scar	Scar sites	Epicardial VT-related	*P*-value[a]	Optimal cutoff[a]	AUC (95% CI)[a]	Sensitivity[a]	Specificity[a]
ARVC ($n = 1664$)								
TAI, ms	4 (−1–10)	3 (−7–12)	26 (7–49)	<0.001	17 ms	0.78 (0.71–0.83)	70%	82%
MAI, ms	20 (14–28)	22 (12–37)	63 (38–85)	<0.001	45 ms	0.80 (0.75–0.84)	73%	81%
EIAR ($n = 905$)								
TAI, ms	3 (−2–9)	2 (−6–7)	44 (30–75)	<0.001	27 ms	0.99 (0.98–0.99)	100%	97%
MAI, ms	22 (15–30)	26 (16–44)	86 (47–113)	<0.001	46 ms	0.91 (0.86 0.96)	100%	77%

Variables are expressed as median (IQR). ARVC denotes arrhythmogenic right ventricular cardiomyopathy; CI, confidence interval; EIAR, exercise-induced arrhythmogenic remodelling; TAI, transmural activation interval; MAI, maximal activation interval.
[a]For differentiation between epicardial VT-related sites and scar sites.

Discussion

The present study is the first to systematically analyse the TAI during SR at VT-related sites in patients with RV cardiomyopathies and predominantly hemodynamically non-tolerated VT. Prolonged TAI and MAI allowed more accurate identification of areas harbouring the VT substrate compared with voltage and local EGM duration criteria. TAI and MAI are novel and voltage independent mapping tools to identify subepicardial areas critical for VT, and may facilitate substrate-based ablation at the epicardial RV.

Substrate-based ablation strategies in right ventricular cardiomyopathy

In patients with RVCM undergoing VT ablation, up to 68% of induced VTs are hemodynamically not tolerated and require substrate-based ablation strategies.[2] In line with this data, the vast majority of patients in our cohort had fast, not tolerated VT. VTs are typically due to scar-related re-entry often confined to the subepicardium.[1–5] Delineation of the affected areas by conventional voltage mapping can be difficult. The amplitude of epicardial BV can be attenuated by overlying fat and other anatomical obstacles. Approximately 65% of the epicardial surface is covered by some degree of fat and 25% is covered by >4 mm of fat, in particular at the RV free wall towards the RV groove.[8] Of note, this peri-tricuspid region is often affected early in the disease and a common location of the VT substrate in ARVC.[3,11]

Because of the epicardial fat layer and the coronary arteries, different epicardial BV cut-off values to identify scar have been suggested: < 1.0 mV plus abnormal EGM and <1.5 mV regardless of the EGM morphology in areas without fat.[10,12,13] Endocardial UV mapping has been suggested to delineate subepicardial or intramyocardial scar.[10,12]

However, both UV and BV depend on wall thickness.[14] A recent study from our group could demonstrate that both endocardial UV and BV values are dependent on the location within the RV, likely because of the differences in wall thickness and the influence of adjacent structures.[15] As a consequence, endocardial and epicardial voltage cut-off values to delineate scar have important limitations at the RV and voltage independent tools are desirable to facilitate substrate-based ablation in RVCM.

Ventricular tachycardia-related sites and transmural activation in right ventricular cardiomyopathy

The high incidence of critical isthmus sites at the subepicardium in RV cardiomyopathies suggests the presence of intramural barriers protecting the subepicardium from direct transmural activation. In an elegant paper by Jiang *et al.*,[4] simultaneous endocardial and epicardial recordings during hemodynamically tolerated VT demonstrated that re-entrant activity is often completely confined to the epicardium and, importantly, may be separated from opposing endocardial activation. Intramural areas of fixed or functional conduction block that facilitate

re-entry may give rise to delayed transmural activation during SR and may be detected by combined endocardial and epicardial activation mapping.

In a prior study by Haqqani *et al*.,[2] activation delay from endocardial to directly opposing epicardial sites was found to be significantly prolonged in patients with ARVC compared with normal controls. In addition, the epicardial activation pattern was altered in patients with ARVC, often being independent of the endocardial activation, suggesting intramural conduction delay or block.

The present study extends these findings by systematically assessing the relation of TAI at opposite sites with VT-related sites for both hemodynamically tolerated but also for non-tolerated fast VTs. We could demonstrate that a critically prolonged TAI and MAI during SR, determined before ablation, can identify sites that are related to VT, with a higher diagnostic accuracy than conventional substrate mapping based on voltage mapping and local EGM duration. The high diagnostic accuracy of both TAI and MAI, suggests that the transmural conduction delay plays an important role for the VT substrate in RV cardiomyopathies. The additional value of the inlayer (difference between TAI and MAI) conduction delay recorded during SR seems to be limited. For hemodynamically tolerated VTs with identified critical isthmus sites, based on the gold standards entrainment mapping and/or VT termination, the TAI was exceeding the proposed cutoff at all sites whereas the MAI was prolonged at only 67% of the sites. In this context, it is noteworthy that the epicardial EGM duration was normal at 78% of VT-related sites and did not allow to distinguish between VT-related sites and other scar sites. These findings suggest that areas without evident subepicardial inlayer conduction delay during SR can still be critical for VT that depends on intramural activation delay. This supports the general concept that the epicardial substrates are likely to sustain VT if protected from short and direct activation from the opposite endocardium. The majority of VTs were not hemodynamically tolerated, mainly due to the short VT-cycle length. As a consequence, sites potentially related to VT can only be determined by pace-mapping, which was typically performed randomly and independent from the local EGM characteristics. However, the prolonged TAI found at sites potentially related to fast VT and targeted by limited ablation with subsequent non-inducibility of the clinical VT in 95% of the patients, and non-inducibility for any VT in 74% of the patients, suggests that the TAI can indeed identify the substrate for unmappable VTs.

Of interest, these results were not specific for ARVC but were also observed in EIAR, an RVCM that is associated with rapid, scar-related re-entry VT from the epicardial RV outflow tract.[3] Both the TAI and MAI were significantly longer at VT-related sites in EIAR compared with ARVC, which resulted in an excellent diagnostic accuracy of the TAI to detect VT-related sites in EIAR. This finding suggests that the limited subepicardial RVOT scars observed in EIAR have characteristics that prevent direct transmural activation, which predisposes for VT and can be accurately identified by combined endocardial and epicardial mapping.

Clinical implications

Assessment of transmural activation is a novel mapping tool that may be used to guide VT ablation in patients with RVCM. TAI may be particularly useful for identification of the substrate for hemodynamically unstable VT. The limitations of voltage mapping and the fact that 78% of VT-related sites showed a normal epicardial EGM duration underscore the need for more accurate mapping tools to identify VT-related sites in RVCM. With the current development of software algorithm that allow automatically annotation of LAT, direct visualization of the transmural activation time can be implemented in three-dimensional mapping systems, which currently requires post-processing of the mapping data (see Supplementary material online, *Figure S1*). Future studies are needed to validate the cut-off values in a prospective cohort.

Limitations

The study was retrospective and only patients undergoing EAM for VT ablation were enrolled. Only a minority of VT circuits were mapped, therefore it cannot be excluded that some areas without prolonged TAI and MAI were critical for VT circuits. The presence of intramural scar components in the thin-walled RV could not be proven by CMR due to its limited spatial resolution, and pathology specimens were not available. The density of TAI/MAI points was insufficient to measure surface areas. Multi-site endocardial pacing was not performed to not further prolong the procedural time. If pacing improves substrate detection is unclear.

Conclusion

This is the first study to systematically evaluate TAIs and MAIs in SR in patients with RVCM and predominantly hemodynamically non-tolerated VT. A TAI >17 ms and an MAI >45 ms can identify a protected subepicardial VT substrate. TAI mapping may be an important new mapping tool, independent from voltage criteria and epicardial EGM characteristics to facilitate substrate-based ablation.

Supplementary material

Supplementary material is available at *Europace* online.

Acknowledgements

None.

Funding

The department of cardiology of LUMC received investigator-initiated research funding from Biosense Webster.

Conflict of interest: None declared.

Data availability

The data that support the findings of this study are available from the corresponding author (K.Z.) upon reasonable request.

References

1. Garcia FC, Bazan V, Zado ES, Ren JF, Marchlinski FE. Epicardial substrate and outcome with epicardial ablation of ventricular tachycardia in arrhythmogenic right ventricular cardiomyopathy/dysplasia. *Circulation* 2009;**120**:366–75.
2. Haqqani HM, Tschabrunn CM, Betensky BP, Lavi N, Tzou WS, Zado ES *et al.* Layered activation of epicardial scar in arrhythmogenic right ventricular dysplasia: possible substrate for confined epicardial circuits. *Circ Arrhythm Electrophysiol* 2012;**5**:796–803.
3. Venlet J, Piers SR, Jongbloed JD, Androulakis AF, Naruse Y, den Uijl DW *et al.* Isolated subepicardial right ventricular outflow tract scar in athletes with ventricular tachycardia. *J Am Coll Cardiol* 2017;**69**:497–507.
4. Jiang R, Nishimura T, Beaser AD, Aziz ZA, Upadhyay GA, Shatz DY *et al.* Spatial and transmural properties of the reentrant ventricular tachycardia circuit in arrhythmogenic right ventricular cardiomyopathy: simultaneous epicardial and endocardial recordings. *Heart Rhythm* 2021;**18**:916–25.
5. Philips B, te Riele AS, Sawant A, Kareddy V, James CA, Murray B *et al.* Outcomes and ventricular tachycardia recurrence characteristics after epicardial ablation of ventricular tachycardia in arrhythmogenic right ventricular dysplasia/cardiomyopathy. *Heart Rhythm* 2015;**12**:716–25.
6. Marcus FI, McKenna WJ, Sherrill D, Basso C, Bauce B, Bluemke DA *et al.* Diagnosis of arrhythmogenic right ventricular cardiomyopathy/dysplasia: proposed modification of the task force criteria. *Eur Heart J* 2010;**31**:806–14.
7. Bhonsale A, Groeneweg JA, James CA, Dooijes D, Tichnell C, Jongbloed JD *et al.* Impact of genotype on clinical course in arrhythmogenic right ventricular dysplasia/cardiomyopathy-associated mutation carriers. *Eur Heart J* 2015;**36**:847–55.
8. van Huls van Taxis CF, Wijnmaalen AP, Piers SR, van der Geest RJ, Schalij MJ, Zeppenfeld K. Real-time integration of MDCT-derived coronary anatomy and epicardial fat: impact on epicardial electroanatomic mapping and ablation for ventricular arrhythmias. *JACC Cardiovasc Imaging* 2013;**6**:42–52.

9. Piers SRD, van Huls van Taxis CF, Tao Q, van der Geest RJ, Askar SF, Siebelink HM *et al.* Epicardial substrate mapping for ventricular tachycardia ablation in patients with non-ischaemic cardiomyopathy: a new algorithm to differentiate between scar and viable myocardium developed by simultaneous integration of computed tomography and contrast-enhanced magnetic resonance imaging. *Eur Heart J* 2013;**34**: 586–96.
10. Venlet J, Piers SRD, Kapel GFL, de Riva M, Pauli PFG, van der Geest RJ *et al.* Unipolar endocardial voltage mapping in the right ventricle: optimal cutoff values correcting for computed tomography-derived epicardial fat thickness and their clinical value for substrate delineation. *Circ Arrhythm Electrophysiol* 2017;**10**:e005175.
11. Te Riele AS, James CA, Philips B, Rastegar N, Bhonsale A, Groeneweg JA *et al.* Mutation-positive arrhythmogenic right ventricular dysplasia/cardiomyopathy: the triangle of dysplasia displaced. *J Cardiovasc Electrophysiol* 2013;**24**:1311–20.
12. Polin GM, Haqqani H, Tzou W, Hutchinson MD, Garcia FC, Callans DJ *et al.* Endocardial unipolar voltage mapping to identify epicardial substrate in arrhythmogenic right ventricular cardiomyopathy/dysplasia. *Heart Rhythm* 2011;**8**:76–83.
13. Tokuda M, Tedrow UB, Inada K, Reichlin T, Michaud GF, John RM *et al.* Direct comparison of adjacent endocardial and epicardial electrograms: implications for substrate mapping. *J Am Heart Assoc* 2013;**2**:e000215.
14. Glashan CA, Androulakis AFA, Tao Q, Glashan RN, Wisse LJ, Ebert M *et al.* Whole human heart histology to validate electroanatomical voltage mapping in patients with non-ischaemic cardiomyopathy and ventricular tachycardia. *Eur Heart J* 2018;**39**:2867–75.
15. Hoogendoorn JC, Sramko M, Venlet J, Siontis KC, Kumar S, Singh R *et al.* Electroanatomical voltage mapping to distinguish right-sided cardiac sarcoidosis from arrhythmogenic right ventricular cardiomyopathy. *JACC Clin Electrophysiol* 2020;**6**: 696–707.

Corrigendum

https://doi.org/10.1093/europace/euac227
Online publish-ahead-of-print 15 December 2022

Corrigendum to: How to use digital devices to detect and manage arrhythmias: an EHRA practical guide

This is a corrigendum to: Emma Svennberg, Fleur Tjong, Andreas Goette, Nazem Akoum, Luigi Di Biase, Pierre Bordachar, Giuseppe Boriani, Haran Burri, Giulio Conte, Jean Claude Deharo, Thomas Deneke, Inga Drossart, David Duncker, Janet K Han, Hein Heidbuchel, Pierre Jais, Marcio Jansen de Oliveira Figueiredo, Dominik Linz, Gregory Y H Lip, Katarzyna Malaczynska-Rajpold, Manlio F. Márquez, Corrette Ploem, Kyoko Soejima, Martin K Stiles, Eric Wierda, Kevin Vernooy, Christophe Leclercq, Christian Meyer, Cristiano Pisani, Hui Nam Pak, Dhiraj Gupta, Helmut Pürerfellner, H J G M Crijns, Edgar Antezana Chavez, Stephan Willems, Victor Waldmann, Lukas Dekker, Elaine Wan, Pramesh Kavoor, Mohit K Turagam, Moritz Sinner, How to use digital devices to detect and manage arrhythmias: an EHRA practical guide, *EP Europace*, Volume 24, Issue 6, June 2022, Pages 979–1005, https://doi.org/10.1093/europace/euac038

In the originally published version of this manuscript, the names of authors Marcio Jansen de Oliveira Figueiredo and Manlio F. Márquez were incorrectly given.

Both names have now been corrected online.

In addition, the following affiliation was inadvertently omitted for author Manlio F. Márquez: Cardiology, Electrophysiology Service, American British Cowdray Medical Center, Mexico City, México

This affiliation has now been added to the online version of the manuscript as affiliation 27 and all subsequent affiliations in this manuscript affected by this change have been updated accordingly.